Author/s:
Weber, DK;Sani, MA;Gehman, JD

Title:
A routine method for cloning, expressing and purifying Aβ(1-42) for structural NMR studies

Date:
2014-01-01

Citation:
Weber, D. K., Sani, M. A. & Gehman, J. D. (2014). A routine method for cloning, expressing and purifying Aβ(1-42) for structural NMR studies. Amino Acids, 46 (10), pp.2415-2426. https://doi.org/10.1007/s00726-014-1796-x.

Persistent Link:
https://hdl.handle.net/11343/283290

Title

A routine method for cloning, expressing and purifying Aβ(1-42) for structural NMR studies

Authors

1. Daniel K. Weber[a],
2. Marc-Antoine Sani[a],
3. John D. Gehman[a,b] (Corresponding Author)

[a] School of Chemistry, Bio21 Institute, University of Melbourne, Victoria, Australia

[b] GehmanLab, Woodend, Victoria, Australia (current address)

Corresponding Author: John D Gehman jgehman@gehmanlab.com +61 407 536 585

Abstract

Nuclear magnetic resonance (NMR) is a key technology in the biophysicist's toolbox for gaining atomic-level insight into structure and dynamics of biomolecules. Investigation of the amyloid-β peptide (Aβ) of Alzheimer's Disease is one area where NMR has proven useful, and holds even more potential. A barrier to realizing this potential, however, is the expense of the isotopically enriched peptide required for most NMR work. Whereas most biomolecular NMR studies employ biosynthetic methods as a very cost-effective means to obtain isotopically enriched biomolecules, this approach has proven less than straightforward for Aβ. Furthermore, the notorious propensity of Aβ to aggregate during purification and handling reduces yields and increases the already relatively high costs of solid phase synthesis methods. Here we report our biosynthetic and purification developments that yield pure, uniformly enriched ^{15}N and $^{13}C^{15}N$ Aβ(1-42), in excess of 10 mg/L of culture media. The final HPLC-purified product was stable for long periods, which we characterize by solution-state NMR, thioflavin-T assays, circular dichorism, electrospray mass spectrometry, and dynamic light scattering. These developments should facilitate further investigations into Alzheimer's Disease, and perhaps misfolding diseases in general.

Key words

Recombinant peptide, uniform labeling, amyloid beta peptide, Alzheimer’s disease, protein NMR, SUMO, thioflavin T assay, circular dichroism.

Abbreviations

Aβ amyloid beta peptide; APP, amyloid precursor protein; CD, circular dichroism; CV, column volume; DLS, dynamic light scattering; ESI-MS, electrospray ionization mass spectrometry; Gdm.HCl, guanidine hydrochloride; GFP, green fluorescent protein; HSQC, heteronuclear single quantum coherence; IPTG, isopropyl β-D-1-thiogalactopyranoside; LB, lysogeny broth; LC-MS, liquid chromatography-mass spectrometry; MAP, methionine aminopeptidase; NMR, nuclear magnetic resonance; Ni-NTA, nickel-nitrilotriacetic acid; PTM, post-translational modification; ROS, reactive oxygen species; RP-HPLC, reverse-phase high-performance liquid chromatography; RT, room temperature; SPPS, solid phase peptide synthesis; SUMO, small ubiquitin-like modifier; TB, terrific broth; TEV, Tobacco Etch Virus protease; and Ub, ubiquitin.

Introduction

Extracellular neuronal deposits predominantly composed of insoluble fibrillar structures of amyloid beta peptides are ubiquitous in Alzheimer's disease (AD) pathology. These peptides, varying from 39 to 43 residues in length, originate from proteolytic processing of the amyloid precursor protein (APP) (1), whereby production biased towards the highly amyloidogenic 42-residue isoform Aβ(1-42) is a significant risk factor towards the onset of AD (2). Mechanistic links of Aβ peptides to neurodegenerative symptoms, however, have been challenging to identify, but are often proposed in relation to metal binding (3), catalytic roles in reactive oxygen species (ROS) generation (4-6) and perturbing interactions towards model lipid membranes (7-11).

Structural data obtained from nuclear magnetic resonance (NMR) has helped to better understand the pathogenicity of Aβ peptides and to inform rational drug design efforts. NMR-based structural models include helical structures in membrane-mimetic solvents or micelles (12-16), predominately unstructured monomers under aqueous conditions at low temperatures (17, 18), and insoluble fibrillar structures rich in beta sheet (19-23). In addition to overcoming the limitations of X-ray diffraction imposed by the non-crystalline and highly polymorphic nature of Aβ peptides, NMR also provides additional information on dynamics, which could be used in conjunction with computational methods to better appreciate the conformational space populated by the peptide in its native, intrinsically disordered state (24-26). Such studies are, however, limited to the availability of an inexpensive source of milligram quantities of peptide, uniformly or selectively labeled with NMR-useful isotopes (i.e. ^{13}C, ^{15}N, ^{2}H, ^{19}F, etc.).

The large quantities of protein needed for structural biology is typically supplied reasonably efficiently by biosynthesis in *E. coli* or other expression systems. The need for ^{15}N and ^{13}C isotopically enriched molecules in NMR involves simple refinement of the growth media to supply only ^{15}N- and/or ^{13}C-enriched metabolic precursors as the sole nitrogen and carbon sources, respectively. Biosynthetic expression of peptides, however, is not quite as

straightforward, and solid phase peptide synthesis is more commonly employed to produce peptide by means of synthetic chemistry. Where just a few nuclei within a peptide are to be labelled, solid phase synthesis is still standard, albeit with increased cost owing to such specialized precursors (27). Uniform labelling of peptide, however, quickly becomes cost-prohibitive by solid phase synthesis. For the Aβ peptide, these problems are particularly acute, given the 40-42 residue length of the peptide, as well as the poor yields of pure, unmodified, and unoxidized material through for which it is infamous (revised by Finder *et al.* (28).

Toward overcoming such limitations, mixed success has been reported with adapting for peptides the fusion-protein approach sometimes applied to problematic proteins. In this approach, recombinant DNA techniques are used to create a fusion protein where a well-behaved protein subunit is both affinity-tagged for purification ease and linked to a protein of interest with a peptide linker plus protease cleavage site, such as for TEV, Factor Xa, or enterokinase. Aβ(1-40) and Aβ(1-42) free of extraneous N-terminal methionine (as is often the case for straight biosynthesis in *E. coli*) or other residues from sloppy protease cleavage has indeed been produced by this approach (28-31). Adaptations of these methods for isotope labeling, however, have only been comprehensively described for the less-amyloidogenic (and less disease-relevant) Aβ(1-40), either providing low (<2 mg/L of culture) or undisclosed final yields (31). This may in part be due to the typical losses in yield owing to the use of specialized minimal growth media compared to high-density media for routine biosynthetic protein production at natural isotopic abundance (30).

In this study we provide a significantly improved protocol for producing entirely native, uniformly ^{15}N and $^{13}C^{15}N$ labeled recombinant Aβ(1-42) at yields exceeding 10 mg per liter of culture. A scheme based on a SUMO fusion partner is utilized, which has demonstrated promising results for expressing Aβ(1-42), albeit only from small scale cultures (32). The potency, reliability and stability of SUMO protease (Ulp1) compared to traditional-used proteases, which are selective to degenerate linkers and required in prohibitive quantities, also provides significant advantages (33). Furthermore, we incorporate several attractive

features including a modular cloning approach for flexibility in producing mutants or other isoforms of Aβ(34), a fast and simple workflow for isolation and purification of amyloid beta from cleavage reactions (28) and a once-off preparation of SUMO-protease (35) sufficient for routine preparative-scale implementation. The chemical and conformational state of the final product is evaluated by electrospray ionization mass spectrometry, solution NMR, thioflavin T assay and circular dichroism techniques.

Materials and Methods

Cloning, expression and purification of SUMO-Aβ(1-42)

The Aβ(1-42) gene was synthesized by PCR according to the codon-optimized sequence and modular approach previously described by Walsh *et al.* (34). Taq DNA polymerase (MyTaq Red Mix, Bioline, Australia) and oligonucleotides, modified for compatibility with 3' overhangs introduced by Taq, sAβa, 5' - GACGCTGAATTCCGTCACGACTCTGGTTACGAAGTTCACCACCAGA - 3'; sAβb, 5' - CACCACCAGAAGCTGGTGTTCTTCGCTGAAGACGTGGGTTCTAACAAGGGTGCT-3'; aAβc, 5' - TTACACAACGCCACCAACCATCAGACCGATGATAGCACCCTTGTTAGA - 3'; aAβ42d, 5' - TTAAGCGATCACAACGCCACCAACCATCAGACCGAT - 3'; sAβfwd, 5' - CAGGTCTCAAGGTGACGCTGAATTCCGTCAC - 3'; and aAβ42rev, 5' - CAGGTCTCTCTAGATTTAAGCGATCACAACGCC - 3' (Micromon, Australia) were use to construct the gene (see Fig. 1) with BsaI and XbaI restriction sites for subsequent cloning into a pE-SUMOpro expression vector (T7, ampicillin; LifeSensors, Malvern, PA, USA). The construct, encoding a 6-His-tagged SUMO fused to the N-terminus of Aβ(1-42), was propagated using *E. coli* DH5α subcloning cells (Invitrogen) and verified by colony PCR and DNA sequencing (Applied Genetic Diagnostics, University of Melbourne, Australia).

For expression of unlabeled (natural abundance) SUMO-Aβ(1-42), a single colony of freshly transformed *E. coli* One Shot BL21(DE3) expression cells (Invitrogen), selected from a LB agar plate (including 100 µg/mL ampicillin), were used to inoculate LB-Miller overnight

starter-cultures. Day cultures of 500 mL LB-Miller (including 100 µg/mL ampicillin) were then inoculated from 5 mL of starter-culture (OD_{600} 1.5) and grown at 37°C with 275 RPM shaking. Cells were induced with 1 mM IPTG once the OD_{600} reached 0.6 (~3.5 hrs). Growth continued for 4 hrs (OD_{600} 1.4) before cells were harvested by centrifugation (8000 g, 10 min, 4°C). Pellets were snap-frozen with N_2 (l) and stored at -20°C (3.1 g/L culture wet cell mass).

Uniformly labeled ^{15}N and $^{13}C^{15}N$ SUMO-Aβ(1-42) were expressed from cultures grown in Neidhardt's minimal media (36), with 0.52 g/L $^{15}NH_4Cl$ and 5.2 g/L [U-^{13}C]-glucose (Cambridge Isotope Laboratories) being the sole nitrogen and carbon sources, respectively. The culture media (including 100 µg/mL ampicillin) were freshly prepared using the method described by Gehman *et al.* (2008) (37), and sterile-filtered immediately prior to use. Cultures expressing ^{15}N SUMO-Aβ(1-42) were grown as described above for natural-abundance cultures and harvested 4 to 5 hours post-induction (OD_{600} 1.1), yielding wet cell masses of 3.0 g/L of culture. For expression of $^{13}C^{15}N$ SUMO-Aβ(1-42), cells were initially grown in ^{15}N-enriched media with natural abundance glucose and centrifuged (8000 g, 10 min, 4°C) once the OD_{600} reached 0.6. Pellets were resuspended in fresh $^{13}C^{15}N$-enriched media, induced at an OD_{600} 0.8, then harvested 4 to 5 hours after induction (OD_{600} 2.1) to yield a wet cell mass of 5.5 g/L of culture.

Hexahistidine-tagged SUMO-Aβ(1-42), as reported in pilot-scale work by Satakarni and Curtis (32), was found to accumulate in inclusion bodies when expressed in *E. coli*. Accordingly, frozen cell pellets were suspended into denaturing lysis buffer (6 M Gdm.HCl, 100 mM sodium phosphate, 10 mM tris, pH 8.0; 10 mL per 1 g wet cell mass) and sonified on ice to aid lysis (Branson 250; 50% duty cycle, level 5 output). The crude lysate was stirred on ice for 1 hr then clarified by centrifugation (10 000 g, 30 min, RT). The supernatant was applied to a Ni-NTA agarose resin (Qiagen; 10 mL bed volume per 1.3 g of wet cell mass) and then washed with 10 column volumes (CVs) of denaturing buffer (8 M urea, 100 mM sodium phosphate, 10 mM tris, pH 8.0). The fusion protein was refolded on the resin by exchange into 100% native buffer (50 mM sodium phosphate, 300 mM NaCl, pH 8.0) over 4 CVs, increasing concentration stepwise at 25%/CV from denaturing buffer, then washing with

a further 10 CVs of 100% native buffer. Elution took place over 4 CVs of elution buffer (50 mM sodium phosphate, 300 mM NaCl, 250 mM imidazole, pH 8.0) and the protein stored at 4°C. All purification steps with urea were done using chilled buffers as a precaution against possible carbamylation modifications. Purities of 60-90% were determined from SDS-PAGE. Higher purity (>90%) could be obtained using wash buffers at pH 6.3 (denaturing) or containing 20 mM imidazole (native), but not without significant losses from premature elution of protein. Accounting for impurities, final yields of unlabeled, ^{15}N and $^{15}N^{13}C$ SUMO-Aβ(1-42) were 96, 96 and 181 mg/L of culture, respectively, as determined by Bradford assay (38) using Bovine serum albumin (Sigma) as a standard.

Cleavage and purification of Aβ(1-42)

SUMO-Aβ(1-42) (~100 μM), freshly eluted from Ni-NTA resin, with 2 mM DTT added, was cleaved by Ulp1 (preparation described below), at 1000:1 substrate to enzyme molar ratio, for 1-3 days at 4°C. Aggregation was induced by carefully lowering the pH to between 6.5 and 7.0 with 1 M HCl and subsequent incubation at 37°C for 3 hours. Aβ(1-42) was then pelleted by centrifugation (10 000 g, 15 min, RT) and dissolved into 8 M Gdm.HCl or 70% formic acid (~5 mg/mL peptide). Aβ(1-42) was purified by HPLC using a preparative Phenomenex Jupiter C4 column (150 x 21.2 mm, 10 μm particle size, 300 Å pore), maintained at 60°C using a Phenomenex Thermosphere TS-430 column heater. Sample was injected at a 2 mL/min flow rate of TFA (0.1%) and acetonitrile (10%) over 5 minutes, and eluted at 10 mL/min flow using a 20 to 90% linear gradient of acetonitrile over 30 min. Elution volumes were lyophilized and stored at -20°C. Yields of lyophilized unlabeled, ^{15}N and $^{13}C^{15}N$ Aβ(1-42) were 13, 12, and 22 mg/L of culture, respectively, equating to ~40% of the yield expected from quantities of SUMO-Aβ(1-42) purified from cell masses.

Cloning, expression and purification of SUMO protease

DNA encoding residues 403 to 621 of *Saccharomyces cerevisiae* Ulp1 (SUMO Protease 1), with a hexahistidine tag on both the N and C termini (35), was obtained by gene synthesis

(GeneArt, Invitrogen) and codon-optimized using the GeneOptimizer tool supplied. The gene was subsequently cloned into a pET21a(+) expression vector (Novagen) using NdeI and XhoI restriction sites on the N and C terminus, respectively, and propagated using *E. coli* DH5αsubcloning cells (Invitrogen).

For expression, sequence-verified plasmid (Applied Genetic Diagnostics, University of Melbourne, Australia) was freshly transformed into *E. coli* One Shot BL21(DE3) expression cells (Invitrogen). Cells were grown in LB-Miller media (including 100 g/mL ampicillin) at 37°C with 275 RPM shaking. Expression was induced with 1 mM IPTG once OD_{600} reached 0.6, and growth continued for a further 4 hr (OD_{600} 1.8). Cells were harvested by centrifugation (8000 g, 10 min, 4°C), frozen with N_2 (l) and stored at -20°C (5.9 g/L of culture wet cell mass).

For purification, frozen cell pellets were resuspended into native buffer (50 mM sodium phosphate, 300 mM NaCl, 10 mM imidazole, 2 mM DTT, pH 8.0) and lysed by sonification (Branson 250, 50% duty cycle, level 5 output), on ice, with 15 cycles of 30 s bursting and 30 s cooling periods. The lysate was clarified by centrifugation (10 000 g, 15 min, 4 °C), and the supernatant loaded onto Ni-NTA resin (Qiagen). The resin was washed with 10 column volumes (CVs) of native buffer containing 20 mM imidazole and eluted with 350 mM imidazole. Fractions with Ulp1 were pooled, diluted 2-fold with 100% glycerol and stored at -20 °C. The product was confirmed by LC-MS (SGE ProteCol C18, 150.0 x 2.0 mm, 5 µm particle size, 120 Å pore) using a formic acid (0.1%) flow rate of 0.25 mL/min and a linear gradient of 5 to 90% MeCN over 10 min. The average mass was 27 250.24 Da (27 249.96 amu theoretical). Yields of 60 mg/L of culture were determined using a theoretical extinction coefficient at 280 nm (28 590 M^{-1} cm^{-1}).

Mass spectrometry

All mass spectrometry was done using an Agilent TOF 6220 equipped with a dual spray electrospray ionization source. Data were recorded between 100 and 3200 m/z, in positive-

ion mode with 4000 V capillary voltage, 250 V fragmentor voltage for protein samples (or 200 V for peptide), 65 V skimmer voltage, 250 V octopole voltage, 35 psi nebulizer pressure, and 7.0 L/min N_2 drying gas flow at 325 °C. All spectra were analyzed using Agilent MassHunter Qualitative Analysis Software (Version B.05.00, Build 5.0.519.0).

NMR spectroscopy

Lyophilized recombinant Aβ(1-42), between 1 and 2 mg, was dissolved into 500 µL of 10% NH_3 with vortexing and 5 mins bath-sonication, then lyophilized. The peptide was re-dissolved into 60 µL of 50 mM NaOH and then made to 600 µL to consist of buffer (15 mM sodium phosphate, 55 mM NaCl, pH 7.4) and 10% D_2O. The pH was carefully corrected to 7.4 (and not adjusted for pD) by addition of HCl and centrifuged (22000 g, 10 min, 4°C) to remove any aggregated material. The concentration of the supernatant was checked by absorbance at 214 nm using a theoretical coefficient (39) of 76 848 M^{-1} cm^{-1}, and the sample loaded into an ice-cold NMR tube. Sample concentrations typically varied between 200 to 600 µM.

NMR spectra were acquired using a cryoprobe-equipped Bruker 500 MHz Avance II spectrometer. Measurements were made at 5°C, in which the sample could remain soluble for over one week without any visible aggregation or detectable loss in signal. Full backbone chemical shift assignments were made using ^{15}N-HSQC, HNCO and HNCACB spectra. The ^{1}H dimensions were referenced directly to trimethylsilyl propionate-d4 (TSP-d4) at -0.12 ppm and ^{15}N and ^{13}C frequencies indirectly by their gyromagnetic ratios (40). Spectra were processed with NMRPipe (41) and analyzed using CCPNmr Analysis (42).

Thioflavin T aggregation assays

Aggregate-free NMR samples were prepared by dissolving lyophilized synthetic (W. M. Keck Facility, Yale University, New Haven, CT) or recombinant Aβ(1-42) into 10% NH_3 at ~1 mg/mL with vortexing and 5 mins bath-sonication. The peptide was then lyophilized and re-dissolved into 5 mM NaOH at ~100 µM then centrifuged (22000 g, 10 min, 4 °C) to remove

any remaining aggregates. The supernatant was then checked by absorbance at 214 nm using and experimentally determined extinction coefficient of 89 665 $M^{-1}cm^{-1}$ for synthetic peptide and a theoretical coefficient for recombinant peptide of 76 848 M^{-1} cm^{-1}, noting that synthetic preparations have been described to have impurities that lead ~20% overestimations of concentration using theoretical coefficients (28). Stocks of Aβ(1-42) were then made to 40 μM in buffer (30 mM sodium phosphate, 100 mM NaCl, pH 7.4) and kept on ice prior to measurements.

Aggregation assays were performed using black, clear-bottom, 96-well plates (Greiner, Fluotrac 600). Wells were prepared to a total volume of 200 μL and comprised of 10 μM Aβ(1-42) and 20 μM thioflavin T (ThT, Sigma-Aldrich, St Louis, MO) in buffer. Measurements were made at 37°C using a FLUOstar Optima plate reader with 440 nm and 480 nm excitation and emission filters, respectively. Wells were scanned by bottom-read every 10 mins with 5 s shaking prior to measurements.

Circular dichroism

Circular dichroism (CD) measurements were made using a Chirascan-Plus (Applied Photophysics) spectrometer and recorded in triplicate from 185 – 260 nm with 1 nm step size, 1 nm bandwidth, 1 s time-per-point and 0.1 mm path-length cuvettes. Temperature was incremented stepwise from 5°C to 50°C, with 5 min equilibration time prior to each scan.

Results

Cloning, expression and purification of SUMO-Aβ(1-42)

The Aβ(1-42) gene was synthesized by an adaptation of the PCR-based modular approach described by Walsh *et al.* (34). The protocol required only six oligonucleotides, in which mutations, if desired, can be made by a simple substitution of oligonucleotide components. Adaptions were made to add the required BsaI and XbaI restriction sites for subsequent insertion into the commercial SUMO expression system used, and the oligonucleotide

sequences modified for compatibility with the adenine overhang introduced by Taq DNA polymerase, which, theoretically, also allows direct use of expression systems based upon TA cloning.

SUMO-Aβ(1-42) was expressed from *E. coli* BL21(DE3) cells under control of the T7/lac promoter system, grown from either LB media for natural isotopic abundance, or Neidhardt's minimal media for uniform ^{15}N and ^{13}C labeling. Yields of fusion protein were high (96 mg/L of culture) regardless of culture medium, although an obvious reduction in growth rate was observed for Neidhardt's medium (Fig. 2A). Furthermore, [U-^{13}C]-glucose requirements for $^{13}C^{15}N$ SUMO-Aβ(1-42) were essentially halved by growing cell mass to mid log phase at natural abundance carbon (with ^{15}N-enrichement), followed by resuspension and induction under fully ^{13}C- and ^{15}N-labeled growth conditions, which yielded 181 mg of fusion protein per liter of the final culture.

As prior work has determined that this particular fusion accumulates primarily into inclusion bodies (32), lysis and initial purification steps were done using denaturing buffers. SUMO-Aβ(1-42) was simply isolated by Ni-NTA affinity chromatography on the basis of an N-terminal hexahistidine tag, whereby the use chilled buffers was sufficient for averting risks of carbamylation modifications from urea degradation (43). Furthermore, refolding of the fusion protein was achieved rapidly by on-resin exchange into native buffer, with no loss in yield, purity or cleavage efficiency compared with refolding through 3 days of dialysis (data not shown).

ESI-LCMS revealed the average mass of SUMO-Aβ(1-42) to be 16775 Da (Fig. 2B), exactly 131 Da less than expected and corresponds to the loss of the N-terminal methionine residue, most likely from post-translational modification (PTM) by methionine aminopeptidase (MAP) (44). Average masses for ^{15}N and $^{15}N^{13}C$ SUMO-Aβ(1-42) were measured at 16985 Da and 17691 Da, respectively. Enrichment of ^{15}N was therefore determined to be 99%, and ^{13}C-enrichement of doubly labeled protein was 97% based on the assumption of 99% ^{15}N-enrichment. SDS-PAGE analysis of expressed and purified fusion protein (Fig. 2C) shows the fusion protein to migrate as multiple bands. The apparent molecular weight and intensity

of these extra bands (generally greater for isotope-enriched batches) corresponds well with additional peaks at +178 Da and +258 Da extra mass from ESI-MS spectra (Fig. 2B) and are consistent with addition of *αN*-6-phosphogluconoyl (+258 Da) with subsequent dephosphorylation to *αN*-gluconoyl (+178 Da), which is a common N-terminal PTM for his-tagged fusion proteins (45). Furthermore, the extra masses were identical between natural abundance and ^{15}N-enriched protein, as expected from being a nitrogen-free PTM, while ^{13}C-enrichment of doubly labeled material increased the observable +178 Da mass to +183 Da – roughly consistent (at least within error of mass determination) with six additional ^{13}C atoms.

Cleavage and Purification of Aβ(1-42)

The active unit of SUMO protease 1 (Ulp1) is defined as the amount required to cleave 15 µg of SUMO-M-GFP at 25 °C in 1 hr (33). Accounting for the molar mass of SUMO-Aβ(1-42), a standard reaction with 100 mg of fusion protein would require almost 15000 units of enzyme. Enzyme requirements for routine production of Aβ(1-42) would, therefore, be cost prohibitive with current commercial sources. For this reason, we cloned and expressed a dual-his-tagged catalytic Ulp1(403-621) domain from *Saccharomyces cerevisiae* as reported by Lee *et al.* (35). Expression from *E. coli* BL21(DE3) provided approximately 60 mg of enzyme per liter of culture, in which a single one liter batch provided sufficient enzyme to cleave over 35 g of SUMO-Aβ(1-42) using the protocol described within this paper.

Cleavage of SUMO-Aβ(1-42) was performed at 4°C to reduce risks of Aβ(1-42) aggregation throughout the reaction. Figure 2D shows that an enzyme to substrate molar ratio of 1:10 was sufficient for approximately 75% cleavage over 1 hour at 4°C, which is several orders of magnitude slower than previous reports of complete cleavage at ratios as low as 1:10000 (33). While 4°C is much lower than optimal range of 22 to 37°C, enzyme activity was only expected to be reduced by approximately a factor of two (33). Soluble aggregates, however, were observed and roughly estimated by DLS to have a hydrodynamic radius of 12 nm, with intensity also centered around 200 nm arising from a small population a larger aggregates considering the sixth-power relationship of light scattering intensity to

particle size (Fig. 2E). Therefore, obstruction of the cleavage site may explain the observed enzymatic inefficiencies. Nonetheless, losses in activity were compensated for by an extended cleavage duration, in which periods longer than 24 hours were sufficient for maximal cleavage (~75 %) at a ratio of 1:1000 (Fig. 2C). The tolerance of Ulp1 against high salt and imidazole content allowed cleavage to be done immediately following elution from Ni-NTA resin, i.e. without any need of buffer exchange or pH adjustment. Cleavage at ~100 µM fusion protein occurred without any visible aggregation of liberated Aβ(1-42), even upon heating to 37°C. Subsequent pH-adjustment from 8.0 to between 6.5 and 7.0, with incubation at 37°C for several hours, was required for complete aggregation, at which point centrifugation was convenient to purifying and concentrate Aβ(1-42) from the cleavage mixture.

Non-cleaved fusion protein co-aggregated with Aβ(1-42) and required further purification by preparative RP-HPLC to remove. SUMO-Aβ(1-42) and traces of free SUMO eluted between 15 and 18 minutes, while Aβ(1-42) eluted with a broad profile peaking at 20 minutes (Fig. 3A). The broad elution profile of Aβ(1-42) is consistent with aggregation on the column, which is expected from the highly hydrophobic nature of the peptide. ESI-MS confirmed the mass of unlabeled, ^{15}N- and ^{13}C^{15}N Aβ(1-42) to be 4514.53 Da, 4568.64 Da and 4764.23 Da (Fig. 3B, 3C), respectively, and only trace quantities of non-cleaved fusion protein remaining (Fig. 3C).

Biophysical characterization of Aβ(1-42)

Solution NMR on aqueous preparations was used to confirm the chemical and conformational purity of uniformly-labeled Aβ(1-42). At the high concentrations required, it is strictly necessary that pre-aggregated material are removed; otherwise seeded fibrillization would lead to rapid loss in signal. Ammonia pretreatment, followed by dissolution into sodium hydroxide (46) worked effectively for this purpose. Figure 4 displays a well-resolved HSQC spectrum of monomeric Aβ(1-42). Cross-peak positions are well-matched to previous spectra of either Aβ(1-40) or Aβ(1-42) with similar buffer composition and temperature (18, 30, 31, 47-

52). In addition, samples maintained at 5°C were stable for periods exceeding one week, which allowed confirmation of $^{1}H^{15}N$ HSQC assignments through a longer triple-resonance ^{15}N-edited HNCACB experiment. The absence of the His^{6} amide cross-peak in our HSQC is consistent with spectra reported by Williamson *et al.* (2006) for Aβ(1-40) (47), while our peak positions for residues Val^{36} to Val^{40} display relative downfield shifts, possibly explained by greater beta-sheet propensity in the C-terminus for Aβ(1-42) (18). Resonances for Ala^{2} and Asp^{7} in HSQC spectra, overlapped with Ala^{30} and Asp^{23}, respectively, were assigned directly by reference to Williamson *et al.* (2006), however, it should be noted that our experiments could not confirm this as neither the HN(i)/CαCβ(i-1) or HN(i)/CαCβ(i) correlation was observed in HNCACB spectra for these residues. In other studies, absence of His^{13} and His^{14}, and deviations of Asp^{7}, Asn^{27} and Lys^{28} amide cross-peaks positions, relative to our HSQC spectra also exist (18, 30, 31, 49), and may possibly be explained by differences in sample preparation (i.e. our inclusion of NaCl, and strength of ammonia pretreatment). Furthermore, the Met^{35} chemical shift position suggests that Aβ(1-42) is in the reduced form (18), consistent with ESI-MS characterization (Fig. 3B, 3C).

Thioflavin T assays were used to characterize the aggregation kinetics of recombinant Aβ(1-42). Figure 5A displays a distinct lag phase, elongation phase and stationary phase over a 24-hour incubation period at 37°C for synthetic material, typical of Aβ aggregation (53). In contrast, recombinant peptide displayed negligible increases in ThT fluorescence, suggesting suppression of fibril formation at low concentration (10 μM). At significantly higher concentrations used for NMR (>200 uM), heating samples upwards of 5°C caused rapid loss in signal and visible development of turbidity, which is consistent with fibrillization. Circular dichroism spectra of used NMR sample (5 days old), but stored at no higher than 5°C and with no visible appearance of aggregation, showed evidence of some helical content based upon characteristic minima at 208 and 222 nm. However, the typical lineshape produce by the presence of α-helix should lead to a *ca.* 2-fold greater positive band at 190 nm, which was not observed in Fig 5A. The low intensity may be explained by a high proportion of random coil content producing a strong negative band at 190 nm. Upon heating

from 5°C to 50°C, a two-state transition was observed with an isodichroic point at *ca.* 210 nm. A positive band at 195 nm and a negative band at 218 nm developed during the heating phase, typical of increasing content of β-sheet structures. This is also consistent with the NMR data where increasing the temperature induced a loss of the NMR signal due to aggregation.

Discussion

Here we have utilized a SUMO-Aβ(1-42) fusion for the purpose of routinely producing milligram quantities of ^{15}N and $^{13}C^{15}N$ labeled Aβ(1-42) suitable for NMR studies. Similar to other fusion strategies based on GST, HEL, $(NANP)_{19}$, and MBP partners, which have previously been proven successful for expressing Aβ peptides [19-22], SUMO alleviated insolubility, could be enzymatically cleaved to release entirely native peptide (i.e. no N-Met) without any trace of N-terminal modification, and allowed single-step isolation from cell lysates, in our case from a polyhistidine tag and Ni-NTA affinity chromatography. Furthermore, SUMO does not rely upon tethering via linker sequences specific to proteases such as Factor Xa, EK or TEV, which are required in large quantities and have known instances of infidelity leading to N-terminal artifacts (30, 33). Instead, recognition intrinsic to the structure of SUMO allows SUMO protease to cleave the C-terminus with much greater fidelity and potency (33). For analogous advantages to SUMO, the ubiquitin (Ub)-fused Ub-Aβ(1-42) has also received interest, (54) with improvements in expression and overall yields of Aβ(1-42) realized for the double-fusions GroES-Ub-Aβ(1-42) (55) and trigger factor-Ub-Aβ(1-42) (56), but even under these improved circumstances, yields are only at comparable levels to our work despite the greater degree of complexity required.

The potential benefits of SUMO for expressing the notoriously difficult Aβ(1-42) has also been realized in past work by Satakarni and Curtis (32), which found expression of SUMO-Aβ(1-42), extrapolated from 25 mL scale, to exceed 200 mg/L of culture. Indeed, our values (~100 mg/L of culture) were considerably lower, which may in some part be

associated with the preparative (>1 L) scale of our work, our use of *E. coli* BL21(DE3) instead of an *E. coli* Rosetta (DE3) pLysS expression strain, or possibly differing methods of protein quantification (not explicitly disclosed in prior work (32)). Furthermore, it was realized in our work that significant challenges were associated with using SUMO-Aβ(1-42) for the eventual preparative-scale production of Aβ(1-42). Firstly, despite being considerably more soluble than Aβ(1-42), the fusion construct still localizes primarily in inclusion bodies (32). While this has commonly been observed for other fusion constructs (28, 30, 31, 55), requirements for dissolution into denaturing buffers is undesirable owing to risks of protein modifications (43) and losses in yields and time associated with refolding. Fortunately, SUMO-Aβ(1-42) could be refolded by on-resin buffer exchange, effectively averting days of dialysis. Secondly, and perhaps the most significant barrier to up-scaled application, is that even at the full published activity (33), a typical batch of 100 mg of SUMO-Aβ(1-42) would require ~15000 units of enzyme to process, which by current commercial suppliers would be a cost prohibitive quantity. Furthermore, the activity of Ulp1(403-621), which we expressed by a method adapted from Lee *et al.* (35), was found to be orders of magnitude less than theoretically expected (33), therefore, adding to already-burdensome enzyme requirements. In agreement with Satakarni and Curtis (32), DLS analysis suggested the presence of soluble aggregates, which could have been responsible for reduced enzyme activity and ~25% loss in overall yields of Aβ(1-42) due to non-cleaved fusion protein, albeit this was not an issue for the prior study. Instead, complete cleavage and activity was observed from their reactions in buffer containing 2 M urea and 37°C, which may have destabilized aggregate assemblies to some extent, but would have also introduced risks of carbamylation modifications from urea degradation. For our work, prolonged reactions at 1:1000 molar ratio of enzyme to substrate, at low temperature in native buffer, was an acceptable solution for reduced activity, allowing a single preparation (grown from 1 L of culture) of Ulp1(403-621) to be sufficient hundreds of preparative-scale cleavage reactions.

Overall yields of lyophilized Aβ(1-42) from our work exceeded 10 mg per liter of culture at either natural isotopic abundance with uniformly ^{15}N or $^{13}C^{15}N$ labeling (see Table 1

for summary of yields and ESI-MS analysis). While these yields (of unlabeled peptide) could have been significantly improved by using higher-density growth media over LB (i.e. TB), doing so would have been misleading for the NMR spectroscopist given that similar yields would be unrealistic from culture media commonly used for isotope labeling – as exemplified by Long *et al.* in expressing a GST-Aβ40 fusion, in which a five-fold reduction in yield was observed between TB and M9 media (30). In contrast, our yields of uniformly labeled material from Neidhardt's minimal media were identical to that obtained from LB.

From ESI-MS analysis, Aβ(1-42) was confirmed to be entirely free of Met^{35} oxidation or other PTMs, while solution NMR provided additional confidence that the final product obtained in a native unstructured state, and that chemical shifts were consistent with prior published work (18, 30, 31, 47-52). In addition, the peptide was remarkably stable throughout NMR acquisition, easily providing for at least one week of spectral acquisition despite having near-physiological concentrations of salt present, which have been noted to reduce sample lives to less than 24 hours (47). Furthermore, ThT assays provided further evidence that the recombinant peptide was suppressed from fibrillization relative to synthetic material, which is contrary to the conclusions made by Finder *et al.* that recombinant material aggregates faster as a result of being absent of the synthetic and racemic impurities inherent in SPSS (28). While the exact reasons for this discrepancy are unclear, trace quantities of non-cleaved fusion protein remaining from HPLC purification as result of broad elution profiles, evident from ESI-MS analysis, but not observable in NMR spectra, may have had some chaperoning effect. Overall, utilization of SUMO fusion methodology has proven applicable as a cost-effective means for the large-scale biosynthetic production of isotopically-enriched Aβ(1-42), and possibly amyloidogenic peptides in general.

Acknowledgements

The authors would like to sincerely thank Dr. Nick Williamson, Paul O'Donnell and Michael Leeming for discussions regarding ESI-MS acquisition and analysis, John Karas for advice

456 on HPLC purification, and Professor Anthony Wedd and Dr. Zhiguang Xiao for allowing
457 access to equipment required for cell-culture work.
458
459 **Funding**
460 J. Gehman was partially funded by ARC Future Fellowship FT0991558 for this work. Circular
461 Dichroism and Dynamic Light Scattering instruments were funded by a LIEF grant
462 LE120100186 to G. Bryant (RMIT) and J. Gehman. D. Weber is thankful for an Australian
463 Postgraduate Award PhD scholarship and Dowd Foundation Postgraduate Research
464 Scholarship for Neuroscience.

References

1. Sisodia, S. S. (1992) β-Amyloid precursor protein cleavage by a membrane-bound protease. Proceedings of the National Academy of Sciences of the United States of America 89:6075-6079
2. Selkoe, D. J. (2012) Preventing alzheimer's disease. Science 337:1488-1492
3. Watt, A. D., Villemagne, V. L., and Barnham, K. J. (2012) Metals, membranes, and amyloid-β oligomers: Key pieces in the Alzheimer's disease puzzle? (Perry, G., Zhu, X., Smith, M. A., Sorensen, A., and Avila, J., eds) 3:283-293
4. Butterfield, D. A., and Lauderback, C. M. (2002) Lipid peroxidation and protein oxidation in Alzheimer's disease brain: Potential causes and consequences involving amyloid β-peptide-associated free radical oxidative stress. Free Radical Biology and Medicine 32:1050-1060
5. Barnham, K. J., Haeffner, F., Ciccotosto, G. D., Curtain, C. C., Tew, D., Mavros, C., Beyreuther, K., Carrington, D., Masters, C. L., Cherny, R. A., Cappai, R., and Bush, A. I. (2004) Tyrosine gated electron transfer is key to the toxic mechanism of Alzheimer's disease β-amyloid. FASEB Journal 18:1427-1429
6. Barnham, K. J., Ciccotosto, G. D., Tickler, A. K., Ali, F. E., Smith, D. G., Williamson, N. A., Lam, Y. H., Carrington, D., Tew, D., Kocak, G., Volitakis, I., Separovic, F., Barrow, C. J., Wade, J. D., Masters, C. L., Cherny, R. A., Curtain, C. C., Bush, A. I., and Cappai, R. (2003) Neurotoxic, Redox-competent Alzheimer's β-Amyloid Is Released from Lipid Membrane by Methionine Oxidation. Journal of Biological Chemistry 278:42959-42965
7. Weber, D. K., Gehman, J. D., Separovic, F., and Sani, M. A. (2012) Copper modulation of amyloid beta 42 interactions with model membranes. Australian Journal of Chemistry 65:472-479
8. Gehman, J. D., O'Brien, C. C., Shabanpoor, F., Wade, J. D., and Separovic, F. (2008) Metal effects on the membrane interactions of amyloid-β peptides. European Biophysics Journal 37:333-344
9. Lau, T. L., Gehman, J. D., Wade, J. D., Masters, C. L., Barnham, K. J., and Separovic, F. (2007) Cholesterol and Clioquinol modulation of Aβ(1-42) interaction with phospholipid bilayers and metals. Biochimica et Biophysica Acta - Biomembranes 1768:3135-3144
10. Lau, T. L., Gehman, J. D., Wade, J. D., Perez, K., Masters, C. L., Barnham, K. J., and Separovic, F. (2007) Membrane interactions and the effect of metal ions of the amyloidogenic fragment Aβ(25-35) in comparison to Aβ(1-42). Biochimica et Biophysica Acta - Biomembranes 1768:2400-2408
11. Sciacca, M. F. M., Kotler, S. A., Brender, J. R., Chen, J., Lee, D. K., and Ramamoorthy, A. (2012) Two-step mechanism of membrane disruption by Aβ through membrane fragmentation and pore formation. Biophysical Journal 103:702-710
12. Sticht, H., Bayer, P., Willbold, D., Dames, S., Hilbich, C., Beyreuther, K., Frank, R. W., and Rosch, P. (1995) Structure of amyloid A4-(1-40)-peptide of Alzheimer's disease. European Journal of Biochemistry 233:293-298
13. Coles, M., Bicknell, W., Watson, R. A., Fairlie, D. P., and Craik, D. J. (1998) Solution structure of amyloid β-peptide(1-40) in a water-micelle environment. Is the membrane-spanning domain where we think it is? Biochemistry 37:11064-11077

14. Watson, A. A., Fairlie, D. P., and Craik, D. J. (1998) Solution structure of methionine-oxidized amyloid β-peptide (1-40). Does oxidation affect conformational switching? Biochemistry 37:12700-12706
15. Crescenzi, O., Tomaselli, S., Guerrini, R., Salvadori, S., D'Ursi, A. M., Temussi, P. A., and Picone, D. (2002) Solution structure of the Alzheimer amyloid β-peptide (1-42) in an apolar microenvironment: Similarity with a virus fusion domain. European Journal of Biochemistry 269:5642-5648
16. Tomaselli, S., Esposito, V., Vangone, P., Van Nuland, N. A. J., Bonvin, A. M. J. J., Guerrini, R., Tancredi, T., Temussi, P. A., and Picone, D. (2006) The α-to-β conformational transition of Alzheimer's Aβ-(1-42) peptide in aqueous media is reversible: A step by step conformational analysis suggests the location of β conformation seeding. ChemBioChem 7:257-267
17. Vivekanandan, S., Brender, J. R., Lee, S. Y., and Ramamoorthy, A. (2011) A partially folded structure of amyloid-beta(1-40) in an aqueous environment. Biochemical and Biophysical Research Communications 411:312-316
18. Hou, L., Shao, H., Zhang, Y., Li, H., Menon, N. K., Neuhaus, E. B., Brewer, J. M., Byeon, I. J. L., Ray, D. G., Vitek, M. P., Iwashita, T., Makula, R. A., Przybyla, A. B., and Zagorski, M. G. (2004) Solution NMR Studies of the Aβ(1-40) and Aβ(1-42) Peptides Establish that the Met35 Oxidation State Affects the Mechanism of Amyloid Formation. Journal of the American Chemical Society 126:1992-2005
19. Lührs, T., Ritter, C., Adrian, M., Riek-Loher, D., Bohrmann, B., Döbeli, H., Schubert, D., and Riek, R. (2005) 3D structure of Alzheimer's amyloid-β(1-42) fibrils. Proceedings of the National Academy of Sciences of the United States of America 102:17342-17347
20. Petkova, A. T., Ishii, Y., Balbach, J. J., Antzutkin, O. N., Leapman, R. D., Delaglio, F., and Tycko, R. (2002) A structural model for Alzheimer's β-amyloid fibrils based on experimental constraints from solid state NMR. Proceedings of the National Academy of Sciences of the United States of America 99:16742-16747
21. Petkova, A. T., Yau, W. M., and Tycko, R. (2006) Experimental constraints on quaternary structure in Alzheimer's β-amyloid fibrils. Biochemistry 45:498-512
22. Paravastu, A. K., Leapman, R. D., Yau, W. M., and Tycko, R. (2008) Molecular structural basis for polymorphism in Alzheimer's β-amyloid fibrils. Proceedings of the National Academy of Sciences of the United States of America 105:18349-18354
23. Lu, J. X., Qiang, W., Yau, W. M., Schwieters, C. D., Meredith, S. C., and Tycko, R. (2013) Molecular structure of β-amyloid fibrils in alzheimer's disease brain tissue. Cell 154:1257-1268
24. Sgourakis, N. G., Merced-Serrano, M., Boutsidis, C., Drineas, P., Du, Z., Wang, C., and Garcia, A. E. (2011) Atomic-level characterization of the ensemble of the Aβ(1-42) monomer in water using unbiased molecular dynamics simulations and spectral algorithms. Journal of Molecular Biology 405:570-583
25. Rosenman, D. J., Connors, C. R., Chen, W., Wang, C., and García, A. E. (2013) Aβ monomers transiently sample oligomer and fibril-like configurations: Ensemble characterization using a combined MD/NMR approach. Journal of Molecular Biology 425:3338-3359
26. Ball, K. A., Phillips, A. H., Wemmer, D. E., and Head-Gordon, T. (2013) Differences in β-strand populations of monomeric Aβ40 and Aβ42. Biophysical Journal 104:2714-2724

27. Mehta, A. K., Rosen, R. F., Childers, W. S., Gehman, J. D., Walker, L. C., and Lynn, D. G. (2013) Context dependence of protein misfolding and structural strains in neurodegenerative diseases. Biopolymers 100:722-730
28. Finder, V. H., Vodopivec, I., Nitsch, R. M., and Glockshuber, R. (2010) The Recombinant Amyloid-β Peptide Aβ1-42 Aggregates Faster and Is More Neurotoxic than Synthetic Aβ1-42. Journal of Molecular Biology 396:9-18
29. Hortschansky, P., Schroeckh, V., Christopeit, T., Zandomeneghi, G., and Fändrich, M. (2005) The aggregation kinetics of Alzheimer's β-amyloid peptide is controlled by stochastic nucleation. Protein Science 14:1753-1759
30. Long, F., Cho, W., and Ishii, Y. (2011) Expression and purification of 15N- and 13C-isotope labeled 40-residue human Alzheimer's β-amyloid peptide for NMR-based structural analysis. Protein Expression and Purification 79:16-24
31. Nagata-Uchiyama, M., Yaguchi, M., Hirano, Y., and Ueda, T. (2007) Expression and purification of uniformly 15N-labeled amyloid β peptide 1-40 in Escherichia coli. Protein and Peptide Letters 14:788-792
32. Satakarni, M., and Curtis, R. (2011) Production of recombinant peptides as fusions with SUMO. Protein Expression and Purification 78:113-119
33. Malakhov, M. P., Mattern, M. R., Malakhova, O. A., Drinker, M., Weeks, S. D., and Butt, T. R. (2004) SUMO fusions and SUMO-specific protease for efficient expression and purification of proteins. Journal of Structural and Functional Genomics 5:75-86
34. Walsh, D. M., Thulin, E., Minogue, A. M., Gustavsson, N., Pang, E., Teplow, D. B., and Linse, S. (2009) A facile method for expression and purification of the Alzheimer's disease-associated amyloid β-peptide. FEBS Journal 276:1266-1281
35. Lee, C. D., Sun, H. C., Hu, S. M., Chiu, C. F., Homhuan, A., Liang, S. M., Leng, C. H., and Wang, T. F. (2008) An improved SUMO fusion protein system for effective production of native proteins. Protein Science 17:1241-1248
36. Neidhardt, F. C., Bloch, P. L., and Smith, D. F. (1974) Culture medium for enterobacteria. Journal of Bacteriology 119:736-747
37. Gehman, J. D., Cocco, M. J., and Grindley, N. D. F. (2008) Chemical shift mapping of γ δ resolvase dimer and activated tetramer: Mechanistic implications for DNA strand exchange. Biochimica et Biophysica Acta - Proteins and Proteomics 1784:2086-2092
38. Bradford, M. M. (1976) A rapid and sensitive method for the quantitation of microgram quantities of protein utilizing the principle of protein dye binding. Analytical Biochemistry 72:248-254
39. Kuipers, B. J. H., and Gruppen, H. (2007) Prediction of molar extinction coefficients of proteins and peptides using UV absorption of the constituent amino acids at 214 nm to enable quantitative reverse phase high-performance liquid chromatography-mass spectrometry analysis. Journal of Agricultural and Food Chemistry 55:5445-5451
40. Wishart, D. S., Bigam, C. G., Yao, J., Abildgaard, F., Dyson, H. J., Oldfield, E., Markley, J. L., and Sykes, B. D. (1995) 1H, 13C and 15N chemical shift referencing in biomolecular NMR. Journal of Biomolecular NMR 6:135-140
41. Delaglio, F., Grzesiek, S., Vuister, G. W., Zhu, G., Pfeifer, J., and Bax, A. (1995) NMRPipe: A multidimensional spectral processing system based on UNIX pipes. Journal of Biomolecular NMR 6:277-293
42. Vranken, W. F., Boucher, W., Stevens, T. J., Fogh, R. H., Pajon, A., Llinas, M., Ulrich, E. L., Markley, J. L., Ionides, J., and Laue, E. D. (2005) The CCPN data model for

608 NMR spectroscopy: Development of a software pipeline. Proteins: Structure,
609 Function and Genetics 59:687-696
610 43. Kollipara, L., and Zahedi, R. P. (2013) Protein carbamylation: In vivo modification
611 or in vitro artefact? Proteomics 13:941-944
612 44. Frottin, F., Martinez, A., Peynot, P., Mitra, S., Holz, R. C., Giglione, C., and Meinnel,
613 T. (2006) The proteomics of N-terminal methionine cleavage. Molecular and
614 Cellular Proteomics 5:2336-2349
615 45. Geoghegan, K. F., Dixon, H. B. F., Rosner, P. J., Hoth, L. R., Lanzetti, A. J., Borzilleri,
616 K. A., Marr, E. S., Pezzullo, L. H., Martin, L. B., Lemotte, P. K., McColl, A. S., Kamath,
617 A. V., and Stroh, J. G. (1999) Spontaneous α-N-6-phosphogluconoylation of a 'His
618 tag' in Escherichia coli: The cause of extra mass of 258 or 178 Da in fusion
619 proteins. Analytical Biochemistry 267:169-184
620 46. Ryan, T. M., Caine, J., Mertens, H. D. T., Kirby, N., Nigro, J., Breheney, K.,
621 Waddington, L. J., Streltsov, V. A., Curtain, C., Masters, C. L., and Roberts, B. R.
622 (2013) Ammonium hydroxide treatment of Aβ produces an aggregate free
623 solution suitable for biophysical and cell culture characterization. PeerJ 1, e73
624 47. Williamson, M. P., Suzuki, Y., Bourne, N. T., and Asakura, T. (2006) Binding of
625 amyloid β-peptide to ganglioside micelles is dependent on histidine-13.
626 Biochemical Journal 397:483-490
627 48. Yan, Y., McCallum, S. A., and Wang, C. (2008) M35 oxidation induces Aβ40-like
628 structural and dynamical changes in Aβ42. Journal of the American Chemical
629 Society 130:5394-5395
630 49. Danielsson, J., Andersson, A., Jarvet, J., and Gräslund, A. (2006) 15N relaxation
631 study of the amyloid β-peptide: Structural propensities and persistence length.
632 Magnetic Resonance in Chemistry 44:S114-S121
633 50. Broersen, K., Jonckheere, W., Rozenski, J., Vandersteen, A., Pauwels, K., Pastore, A.,
634 Rousseau, F., and Schymkowitz, J. (2011) A standardized and biocompatible
635 preparation of aggregate-free amyloid beta peptide for biophysical and biological
636 studies of Alzheimers disease. Protein Engineering, Design and Selection 24:743-
637 750
638 51. Rezaei-Ghaleh, N., Andreetto, E., Yan, L. M., Kapurniotu, A., and Zweckstetter, M.
639 (2011) Interaction between amyloid beta peptide and an aggregation blocker
640 peptide mimicking islet amyloid polypeptide. PloS one 6
641 52. Ghalebani, L., Wahlström, A., Danielsson, J., Wärmländer, S. K. T. S., and Gräslund,
642 A. (2012) PH-dependence of the specific binding of Cu(II) and Zn(II) ions to the
643 amyloid-β peptide. Biochemical and Biophysical Research Communications
644 421:554-560
645 53. Sani, M. A., Gehman, J. D., and Separovic, F. (2011) Lipid matrix plays a role in
646 Abeta fibril kinetics and morphology. FEBS Letters 585:749-754
647 54. Lee, E. K., Hwang, J. H., Shin, D. Y., Kim, D. I., and Yoo, Y. J. (2005) Production of
648 recombinant amyloid-β peptide 42 as an ubiquitin extension. Protein
649 Expression and Purification 40:183-189
650 55. Shahnawaz, M., Thapa, A., and Park, I. S. (2007) Stable activity of a
651 deubiquitylating enzyme (Usp2-cc) in the presence of high concentrations of urea
652 and its application to purify aggregation-prone peptides. Biochemical and
653 Biophysical Research Communications 359:801-805
654 56. Thapa, A., Shahnawaz, M., Karki, P., Dahal, G. R., Sharoar, M. G., Shin, S. Y., Lee, J. S.,
655 Cho, B., and Park, I. S. (2008) Purification of inclusion body-forming peptides and

656 proteins in soluble form by fusion to Escherichia coli thermostable proteins.
657 BioTechniques 44:787-796
658

Figure 1: PCR scheme for synthesizing the Aβ(1-42) gene. The modular approach and DNA sequence, codon-optimized for *E. coli*, was identical to that described by Walsh *et al.* (34). The reaction consisted of MyTaq Red Mix, sAβa (600 nM), aAβ42d (600 nM), sAβb (40 nM) and aAβc (40 nM), and underwent 2 cycles of 94°C (15 sec) and 35°C (45 sec); 2 cycles of 94°C (15 sec), 62°C (15 sec) and 64°C (30 sec); and a further 25 cycles of 94°C (15 sec), 66°C (15 sec) and 68°C (15 sec). XbaI and BsaI restriction sites, i.e. if T/A cloning vectors are not used, were then added by a second reaction using a one-tenth dilution of the prior reaction and primers sAβfwd (600 nM) and sAβrev (600 nM), then 2 cycles of 94°C (15 sec), 51°C (15 sec) and 52°C (30 sec); and 25 cycles of 94°C (15 sec), 66°C (15 sec) and 68°C (15 sec).

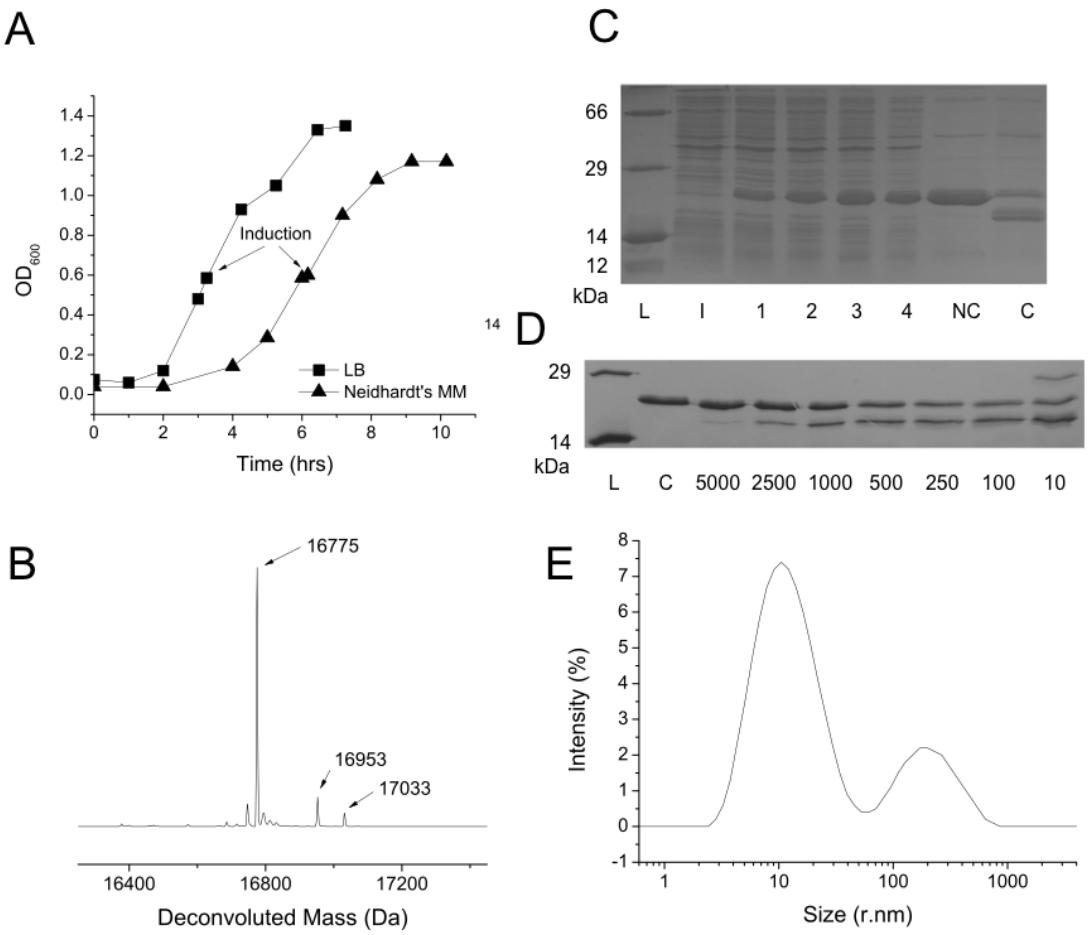

Figure 2: (A) Growth comparison of *E. coli* cultures expressing SUMO-Aβ(1-42) from either LB media or Neidhardt's minimal media used for uniform labeling. (B) Maximum entropy deconvolution of an ESI-MS spectrum of SUMO-Aβ(1-42) at natural isotope abundance. Peaks identified at 16953 and 17033 likely correspond to *α-N*-gluconoyl and *α-N*-6-phosphogluconoyl PTMs, respectively. (C) 15% SDS-PAGE gel of *E. coli* pre- and post-induction of SUMO-Aβ(1-42) expression by IPTG (hours 1-4, lanes 2-6); and Ni-NTA purified SUMO-Aβ(1-42), non-cleaved (NC, lane 7), and cleaved at 1:1000 molar ratio of SUMO protease to fusion protein after 3 days incubation at 4°C in native elution buffer (C, lane 8). (D) Cleavage of 10 μM SUMO-Aβ(1-42) by Ulp1 over 1 hour at 4°C in buffer (50 mM sodium phosphate, 100 mM NaCl, pH 8.0). Molar ratios of SUMO-Aβ(1-42) to protease are displayed below each lane. (E) Size-intensity distribution, proportional to the sixth power of hydrodynamic radius, from dynamic light scattering of SUMO-Aβ(1-42) in elution buffer (50 mM sodium phosphate, 300 mM NaCl, 250 mM Imidazole, pH 8.0, 4°C). Measurements were made using a Malvern Zetasizer Nano ZS in 173° backscatter mode and analyzed by manufacturer's software.

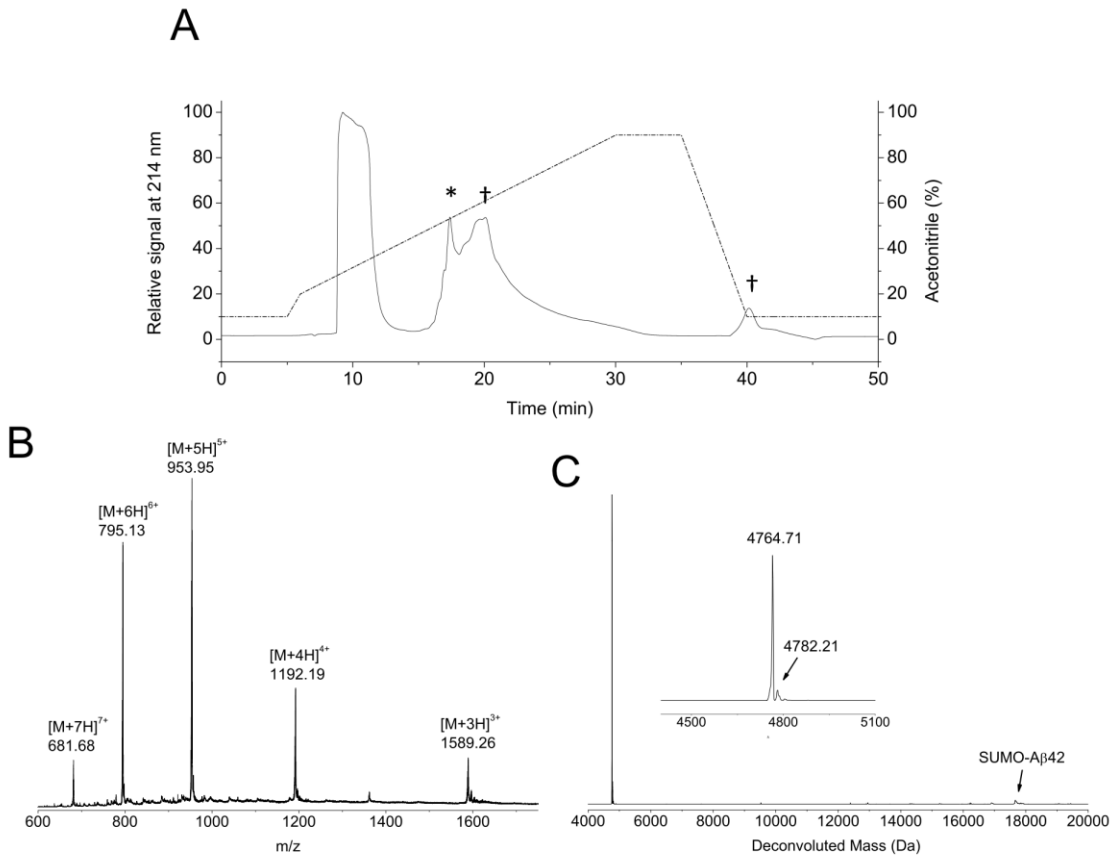

Figure 3: (A) Preparative RP-HPLC elution profile of Aβ(1-42) detected by UV-absorbance (solid line) and showing acetonitrile concentration (dashed line). Peaks are identified corresponding to free SUMO and non-cleaved fusion protein impurities (*) and Aβ(1-42) (†). (B) Raw and (C) maximum entropy deconvolution of ESI-MS spectrum of HPLC-purified $^{13}C^{15}N$ Aβ(1-42). A peak observed at +17.5 Da is consistent with water adducts and not oxidation of Met[35]

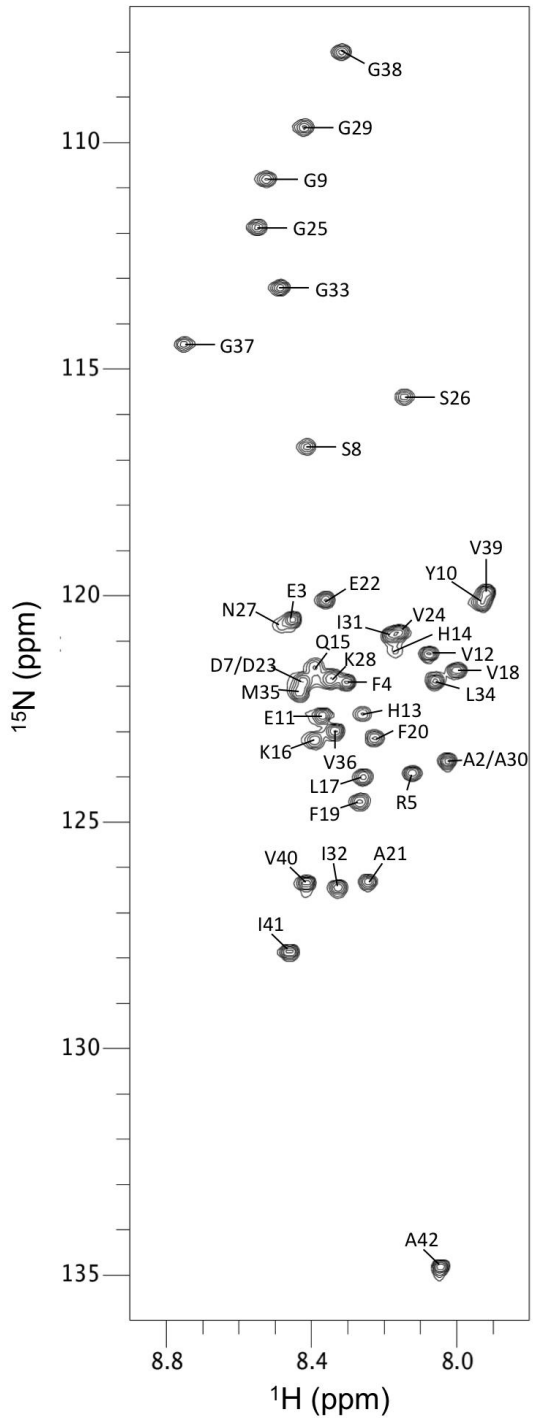

689

690 **Figure 4:** 500 MHz HSQC spectrum of 380 uM $^{13}C^{15}N$ Aβ(1-42) in buffer (15 mM sodium phosphate, 55
691 mM NaCl, pH 7.4) at 5 °C. Spectra were recorded using the standard Bruker hsqcetfpf3gpsi pulse
692 sequence with 10.97 ppm spectral width and 2048 points in the ^{1}H dimension, and 40 ppm spectral
693 width and 256 points in the 15N dimension. Processing was performed using NMRPipe (41) with
694 solvent filtering, sine-bell apodization with maximum shifted to 50% acquisition time, zero filling for
695 both dimensions and forward-back linear prediction for the indirect ^{15}N dimension.

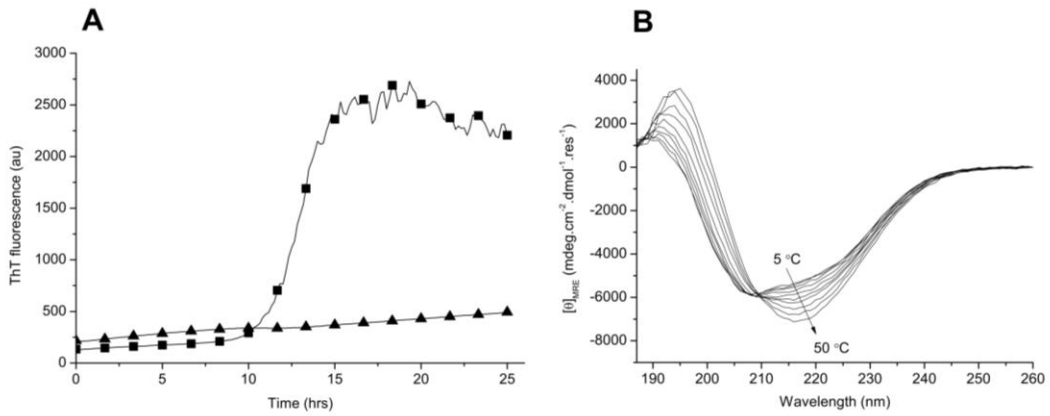

Figure 5: (A) ThT aggregation curve of synthetic (squares) and recombinant (triangles) Aβ(1-42). Samples consisted of 10 uM peptide and 20 uM ThT in buffer (30 mM sodium phosphate, 100 mM NaCl, pH 7.4). Measurements were made at 37°C every 10 minutes. (B) CD spectra of 220 uM $^{13}C^{15}N$ Aβ(1-42) after 5 days of NMR measurements at 5°C. Temperature was incremented to 50°C in steps of 5°C with 5 minutes equilibration prior to each scan.

703 **Table 1**: Summary of yields and ESI-MS confirmation of proteins and peptides produced from this
704 study.

	Experimental M.W. *Da*	**Theoretical M.W.** *Da*	**Enrichment**	**Yield** *(mg/L of culture)*
Ulp1	27250.24	27249.96	-	60
SUMO-Aβ(1-42)	16774.73	16775.03†	-	96
^{15}N SUMO-Aβ(1-42)	16985.16	16987.16†	^{15}N (99%)	96
^{13}C^{15}N SUMO-Aβ(1-42)	17690.91	17717.76†	^{15}N (99%), ^{13}C (97%)	181‡
Aβ(1-42)	4514.53	4514.08	-	13
^{15}N Aβ(1-42)	4568.64	4568.68	^{15}N (99%)	12
^{13}C^{15}N Aβ(1-42)	4764.23	4770.19	^{15}N (99%), ^{13}C (97%)	22‡

705 † Theoretical molecular weights take the loss of N-terminal methionine into account. Additional peaks
706 at 178 Da (Unlabeled, ^{15}N-labeled), 183 Da (^{13}C-labeled), and 258 Da (Unlabeled, ^{15}N-labeled) may
707 appear in ESI-MS spectra and are likely N-terminal αN-gluconoyl and αN-6-phosphogluconoyl PTMs.
708 ‡ Reported yield neglects the volume of culture used to grow cell mass under natural ^{13}C abundance.